Forecasting M6+ 'Significant' Earthquakes (I): The First 100 Days

Ben Davidson[1, 2]
[1] Space Weather News; [2] The Earthquake Prediction Center at QuakeWatch.net
Ben@ObservatoryProject.com, Albuquerque, New Mexico, USA

Abstract: Pre-seismic signals have been identified by numerous studies over the last fifty years. The various signals have been analyzed for numerous large earthquakes. Certain factors (including some not previously studied) stood out as best-suited to indicate impending dangerous seismic activity, and a model was developed for real-world practice of earthquake forecasting. The model demonstrates a highly significant probability of correctly forecasting the region of the next dangerous earthquake to occur. Specific regions and fault systems that would imminently endure M6+ 'significant' earthquakes were identified with +80% accuracy.

1. INTRODUCTION

Foreknowledge of earthquakes dates back to the very first recognition of an aftershock that was caused by a preceding large earthquake nearby. Since then, foreshocks and other phenomena like 'earthquake lights', ground ion emission, and changes total electron content in the atmosphere (TEC) have been recognized as legitimate precursor events to some large earthquakes, but efforts to determine which earthquakes and signals will lead to larger seismic events soon afterwards have fallen short. Active earthquake forecasting remains largely outside of the mainstream lexicon of geophysics.

One of the historical models to demonstrate success in correctly identifying foreshocks and pre-volcanic eruption signals describes how deep earthquakes in the mantle can influence the crust, through a process known as energy transmigration (Blot, 1976; Blot, 1963). Other studies have identified similar patterns in foreshock behavior and other prerequisite conditions prior to large seismic events (Choi and Casey, 2015; Gregori, 2015; Blot, Choi and Grover, 2003; Grover, 1974; Grover, 1967) or recognized long-range to global patterns in how some earthquakes trigger subsequent events (Giacco et al., 2015; Whiteside and Ben-Zion, 1995). In reviewing these patterns, and others accompanying numerous more-recent events, it was observed by Scott Windbiel, and subsequently demonstrated by Windbiel and this author, in an open source/public access format (Windbiel, 2017; Davidson, 2017), that focusing on M4+ earthquakes between the low-velocity zone and the transition zone repeatedly showed a significantly reliable method of narrowing-down an eventual M6+ rupture point over short timescales (less than one week).

In addition to subterranean pre-seismic signals, recent studies have identified numerous atmospheric, ionospheric, magnetospheric, and geospace signals that have preceded large earthquakes. Anomalies in charged particle counts, solar magnetic fields, and in characteristics and radio signals associated with L-shells have been detected before earthquakes (Hayakawa, 2016; Davidson, Holloman, U-yen, 2015; Davidson, 2015; Khachikyan et al., 2014; Fidani et al., 2010), along with other fluctuations of earth's magnetic field. (De Santis et al, 2017; Scoville, 2015; Johnston, 1994). There is a growing body of work on other electromagnetic precursors to earthquakes, like GPS disruptions and TEC fluctuations, and on electric coupling between the ground, atmosphere and ionosphere. (Pulinets, 2014; Kamogawa, 2013; Namgaladze, 2013; Yao, 2012; Zolotov, 2010; Namgaladze, 2009; Rycroft, 2006; Sorokin, 2006; among others). Studies of crustal resistivity can give clues to the structure of the fault, and many fault zones contain low resistivity crustal contents, which might offer a pathway for current. (Iidaka et al., 2015; Morrow et al., 2015; Becken et al., 2011). Models of the earth's crust as a capacitor (Namgaladze, 2013; Ustundag et al., 2005; Hill, 1971) allow fluctuations of the GEC and geomagnetic system to complement known mechanisms for the production of electric currents and other electromagnetic signals before and during earthquakes, including via space weather modulation of geomagnetism, ground currents, vertical electron content and various other aspects of the GEC. In the analysis of these studies, it was observed that atmospheric pressure and thermal outflow (outgoing longwave radiation) were the most reliable indicators of imminent (within 72 hours) crustal ruptures, that the sun-facing side of the earth during space weather impacts presented more deep earthquakes than the night side, and that the deep earthquakes used in this study echo the atmospheric and solar patterns. In honor of Claude Blot, we have termed these deep earthquakes of sufficient magnitude within subducted crust, "Blot echoes".

A model utilizing these observations currently is in constant operation attempting to forecast M6+ 'significant' earthquakes, as defined by the United States Geological Survey. Part I of this communication details the model and forecasting results.

2. THE CURRENT MODEL AND ALERT SYSTEM

Blot echoes are defined in the model as magnitude 4.0 or larger earthquakes at depths of 100 km or deeper. The region immediately above a Blot echo is considered to be at higher risk of M6 or larger seismicity for 72 hours, with a range extending 1000km in every direction, up to 1500km directly along fault systems lying on north/south vectors, and up to 2000km directly along the east/west Indonesia-Oceania fault systems. Subsequent Blot echoes occurring beneath the crustal alert zone of a previous Blot echo reset the 72-hour clock for any unexpired Blot echo alert regions overlapping the one created by the present Blot echo. The progression of the risk over the 72 hours following a Blot echo is dependent on crustal events; M4+ events in the alerted region, occurring shallower than 60km, would indicate that the at least some of it's *crustal disruption potential* indicated by the deep event had been relieved, and would count as an *answer to the Blot echo*, reducing the level of risk for a larger event in that area.

The most robust atmospheric pre-seismic signals involve the wind/pressure and outgoing longwave radiation. Centers of strong low pressure cells, like cyclones and strong extratropical storms, immediately present an increased risk of earthquakes at all depths around most of the ring of fire, central Asia, the Middle east and southern Europe. This risk is confined to a 500km radius. Pressure convergence lines, where the wind collides as it funnels towards the center of low pressure, also provide a similar risk while the line is approaching a subduction zone (within 500km) and for 48 hours after it passes. Surface winds that cross the equator are relevant for South America and eastern Oceania, where risk levels are also elevated at the termination of the trans-equatorial flow (usually occurs at a low pressure cell), and for 500 km along nearby fault systems. As long as any wind- or pressure-driven signals persists overhead, crustal events may be expected and do not necessarily reduce the *crustal disruption potential* of any recent Blot echoes in the region. Outgoing longwave radiation (OLR) is used to gauge the significance of the pressure-driven factors listed above. The strongest gradients in thermal outflow anomalies (Δ >120 W/m-2 in the tropics, Δ >80 W/m-2 outside the tropics) within small geographic areas (less than 12 degrees) indicate the atmospheric pre-seismic signals included in the OLR anomaly gradient merit a high alert.

The regions of earth subject to seismic alert were, and continue to be, posted publicly every 4-36 hours. Regions that contain multiple signals are placed on alert, with more/stronger signals receiving higher alerts, and with a maximum coverage limit of ~20% of the ring of fire, and ~20% of the entire world's active faults. In descending order of alert, we mark with 'alert stars', red lines and yellow lines. Ongoing alerts are recorded and tracked at QuakeWatch.net/statistics along with a full listing of all forecasts made, results, and links to the timestamp-preserved alert posting. (Davidson, 2017). During the period of this study, Twitter was chosen to publicly preserve the forecast timestamps, and which are publicly accessible and likely to be seen (the Twitter user, Ben@TheRealS0s, has +18,000 'followers' and postings were shared on other social media with ~300,000 unique members, followers, viewers, subscribers, etc.). The model is checked after each M6+ 'significant' earthquake. A simple question is asked: Is the most-recently-posted highest level of alert (usually a red line alert or alert star) inclusive of the recent earthquake in question? If yes, the earthquake is a hit for the model. If not, it is a miss. Such simplicity in determining success allows simple binomial probability analysis of the significance of the results, based on how many earthquakes were hits compared to the number expected at random. The current model of forecasting began full-time real-world operation on October 15, 2016. The earthquake forecasting and results of the first 100 days are described below.

3. EXAMPLES OF FORECASTING SUCCESSES AND FAILURES

Italy - M6.6 on October 30, 2016. Despite multiple red line alerts in the ring of fire, the highest alert fell on Italy (alert star, Figure 1) in the alert map posted October 29, 2016. This was the only M6+ main earthquake of the real-world practice period that struck Europe, and it struck the alert star over Italy.

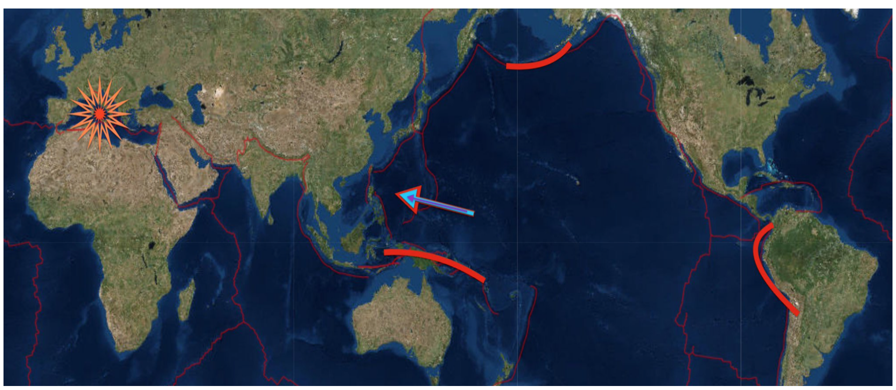

Figure 1: The alert posted most recently before the M6.6 in Italy on October 30, 2016. All Alert Maps were/are produced with the Google satellite image background.

United States - M6.6 on December 8, 2016. The only M6+ event in the United States during real-world practice struck a high alert for the northeast Pacific ring of fire. The other high alert (China) was the recipient of a M6.0 the same day. There were no 'alert stars', therefore the red lines represent the highest alerts that day.

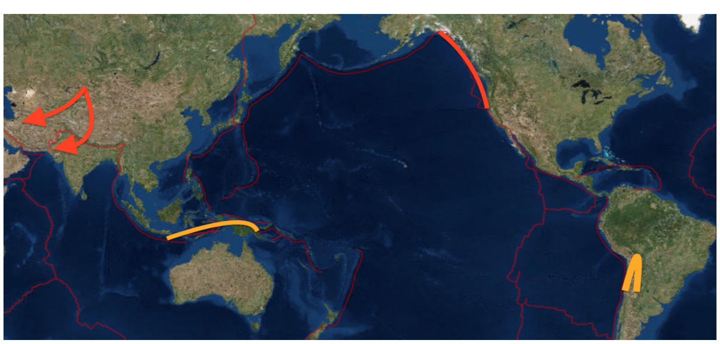

Figure 2: The alert map posted the morning of December 8, 2016.

South America - High Success Rate Throughout Real-World Practice. There were four M6+ 'significant' earthquakes during the first 100 days of real-world practice (M6.3 in Chile on November 4, 2016, M6.4 in northwestern Argentina on November 20, 2016, M6.4 in western Brazil on December 18, 2016, M7.6 in southern Chile on December 25, 2016), each has struck an area on highest alert at that time, and a M6.2 in Peru December 1, 2016 (not 'significant') also occurred within a highest alert area at that time.

Figure 3: The alert map posted most-recently before the November 4, 2016 event.

Japan. There have been three M6+ 'significant' earthquakes in Japan since the real-world practice began, and all three struck during a period when high alerts were in place for the island nation using the system described herein. One example occurred on November 12, 2016, when a M6.1 struck Japan as alert focus fell on the western Pacific (Figure 4).

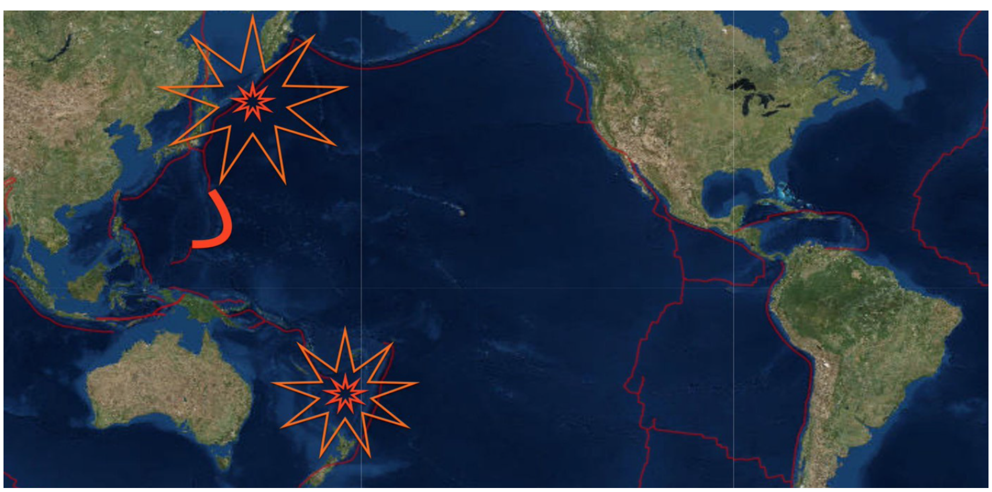

Figure 4: The alert map posted November 11, 2016.

New Zealand - M7.8 on November 13, 2016. After the Japan earthquake on November 12, 2016, focus shifted to the southern ring of fire (Figure 5), with the Oceania alert spreading towards the corners of the fault zones. On November 13, 2016 a M7.8 earthquake struck New Zealand in a high alert zone. The second-largest earthquake of the day, reported by various agencies between M5.8 and M6.2, struck the inland Argentine high alert.

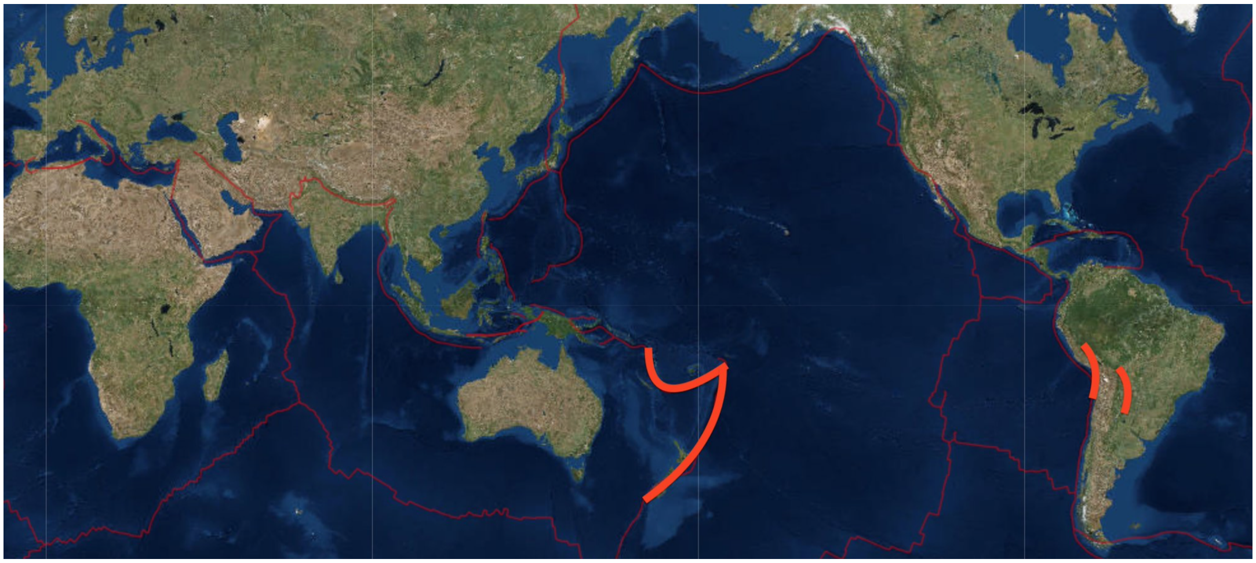

Figure 5: The alert map posted on November 12, 2016 after the M6.1 struck the Japanese alert star (Figure 4).

Missed Earthquake in Tajikistan - M6.6 on November 25, 2016. Only one M6+ ‘significant’ earthquake struck the region where the Middle East meets western Asia in the first 100 days, a M6.6 on November 25, 2016. This area was not on any alert at the time of the earthquake, but a 72-hour high alert based on Blot echoes expired in the region only 72 minutes prior to the earthquake event. While the result is a miss for the model statistics, it offers a clue into the possible wait-time after Blot echoes in this part of the world.

The last Blot echo occurred on November 22, 2016 at 13:12 UTC (Figure 6), and the 72-hour alert expired on November 25, 2016 at 13:12 UTC. The earthquake occurred at 14:24 UTC on November 25, 2016.

Figure 6: Five Blot echoes that struck northwest of India on November 21 and 22, 2016 (top), zoomed-in shot of the Middle East/western Asia alert zone that expired 72 minutes before the earthquake (bottom).

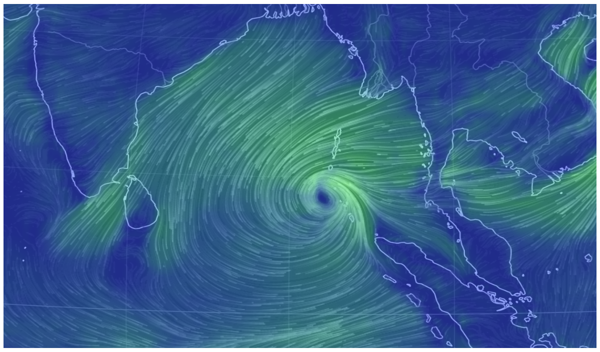

Missed Earthquake in western Indonesia - M6.5 on December 6, 2016. A strong low-pressure cell was off the coast of Aceh, Indonesia in the Indian Ocean. The earthquakes *was* within the factor radius, but the storm itself, without blot echoes, was not enough for a high alert, and the earthquake was not covered.

Figure 8: Low pressure cell northwest of Aceh, Indonesia on December 6, 2016.

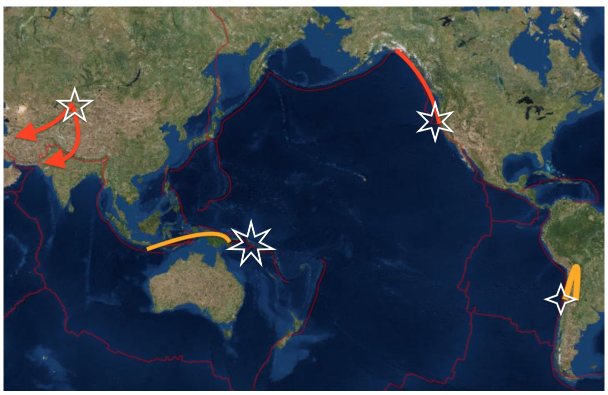

Missed Earthquake in the Solomon Is. - M7.8 on December 8, 2016. On the same day a M6.6 earthquake struck California in high alert zone, a M7.8 struck the Solomon Islands outside the alert. In Figure 9 we see the alert map, with the location of the four largest main earthquakes of the day, including an USA and China events.

Figure 9: Alert map posted for December 8, 2016, with the largest four main earthquake epicenters starred in white.

4. TOTAL MODEL RESULTS, FIRST 100 DAYS (OCTOBER 15, 2016 TO JANUARY 23, 2017)

There were 24 'significant' main (primary) earthquakes larger than M6.0 from October 15, 2016 through January 23, 2017 (the first 100 days). Earthquakes that were clearly foreshocks (Ex: a M6.3 that struck 555 km beneath Fiji one day before a M6.9 struck Fiji in the crust) or aftershocks (Ex: Two M6.5 earthquakes and one M6.2 'significant' earthquake struck New Zealand within 13 hours after the M7.8 on November 13, 2016) were not included. Twenty of these 24 earthquakes (83.3%) struck the highest alert zones of the most recently posted alert map. Alerts covered 17.9% of the world's most-active faults (range, 5-20%), including areas outside of the most-active zones of the ring of fire (Ex: North America, Europe).

Despite covering 17.9% of the active fault areas, there was *some* portion of the fault system spanning from Sumatra to the Kermadec Islands on high alert 71% of the time, and more than 80% of the high alert zones occurred in the ring of fire. The 17.9% of earth covered by the alerts should statistically expect to see between 29% and 37% of the M6+ 'significant' earthquakes, depending on whether one choses historical statistics by country, region, fault zone, or geographic coordinates, and whether 5, 10 or 20 year statistical records are utilized. For the purposes of this analysis, the highest expected success rate at random (37%) was used to create the largest hurdle of significance for this model. At +80% success, the model performs more than 2x better than a random distribution of alert zones.

Using a binomial probability analysis, with the 37% expected success rate, and *n* = 24*,* the mean expected number of earthquakes successfully forecast is 8.88, with a variance of 5.59 and standard deviation of 2.4. At random, the alert zones should cover no more than 14 or 15 of the 24 earthquakes (2 standard deviations). There is a 99.9996% chance of covering fewer than 20 of 24 M6+ 'significant' earthquakes in this time period, using alert zones of this size, and 99.1% probability of covering 14 or less. Table 1 shows every 'significant' earthquake larger than M6.0 in the first 100 days of the forecasting model.

#	Mag.	Date	Location	In Alert Zone?
1	7.9	January 22, 2017	Papua New Guinea	**Alert Zone**
1	7.9	December 17, 2016	Papua New Guinea	**Alert Zone**
3	7.8	November 13, 2016	New Zealand	**Alert Zone**
3	7.8	December 8, 2016	Solomon Is.	**Not in Alert Zone**
5	7.6	December 25, 2016	Chile	**Alert Zone**
6	7.3	January 10, 2017	The Philippines	**Alert Zone**
7	6.9	January 3, 2017	Fiji	**Alert Zone**
7	6.9	November 24, 2016	El Salvador	**Alert Zone**
7	6.9	November 21, 2016	Japan	**Alert Zone**
10	6.8	October 17, 2016	Papua New Guinea	**Not in Alert Zone**
11	6.7	December 20, 2016	Indonesia	**Alert Zone**
12	6.6	December 8, 2016	USA	**Alert Zone**
12	6.6	October 30, 2016	Italy	**Alert Zone**
12	6.6	October 19, 2016	Indonesia	**Alert Zone**
12	6.6	November 25, 2016	Tajikistan	**Not in Alert Zone**
16	6.5	January 19, 2017	Solomon Is.	**Alert Zone**
16	6.5	December 6, 2016	Indonesia	**Not in Alert Zone**
18	6.4	December 18, 2016	Brazil	**Alert Zone**
18	6.4	November 20, 2016	Argentina	**Alert Zone**
20	6.3	December 5, 2016	Indonesia	**Alert Zone**
20	6.3	November 4, 2016	Chile	**Alert Zone**
20	6.3	October 15, 2016	Papua New Guinea	**Alert Zone**
23	6.2	October 21, 2016	Japan	**Alert Zone**
24	6.1	November 11, 2016	Japan	**Alert Zone**

Table 1: The 24 M6+ 'significant' earthquakes that occurred in the first 100 days of real-world model practice of the current earthquake forecasting model, in descending order of magnitude, and whether or not the earthquake struck a high alert zone.

5. DISCUSSION

Restrictive View of Success. Once a M6+ earthquake occurs, *only the most-recently posted alert would count as the alert for the time of the earthquake*. This 'most-recent' rule was employed to simplify understanding of which areas of earth were on alert and which were no longer at risk. With this method, seeking M6+ events, it would theoretically be possible to put Washington D.C. on alert, have five M5.9 earthquakes strike Washington D.C., plus a M6.4 in Georgia, and then one hour after the alert is lifted, a M6.6 could strike Washington D.C., and our model would technically have zero success for the period. This ultimately restrictive view of success was implemented to remove any question as to whether a forecast was successful, even if, as in this example, such an alert would probably merit significant post-study if it were indeed published before such unthinkably rare seismic events.

Informational, Not Actionable. The 17.9% alert zone coverage requires us to characterize the model output as informational, rather than actionable data. Exact locations of earthquakes nearly-guaranteed to occur is not yet achievable, and until the certainty of forecasts matches historical hurricane forecast accuracy, the output should remain informational to avoid unnecessary use of resources, and misunderstandings and inappropriate apprehension among the populace. This model represents one step towards the goal of future earthquake warnings, and one that is necessary for its fulfillment. The potential for negative public reaction resulting from earthquake forecasting should never be an impediment to its progress.

Deviations from Standard Blot-forecasting. Blot echoes have reliably allowed the forecasting of large earthquakes in Europe, South America, Oceania, South/Southeast/Eastern Asia, and Central America. Some regions of the world appear follow slightly different rules. Fault systems of the western United States and Canada do not require the depth of a Blot echo to be a notable foreshock. Occurrences of M4+ events along these coastlines increase the chances that simultaneously occurring atmospheric signals nearby are also pre-seismic signals. In the Middle East, Nepal and southeast Asia, there can be Blot echo events almost daily for continuous months, which do not appear to be as relevant for forecasting large events as certain atmospheric conditions like outgoing longwave radiation (OLR). (this observation is bolstered by Lal and Bhagavathiammal, 2016; Prakesh et al., 2015; and Venkatanathan and Natyaganov, 2014). Large earthquakes in eastern Oceania (Samoa, Tonga, Fiji, Vanuatu, New Caledonia, New Zealand) have much stronger correlation with low-velocity zone Blot echoes than it does with those nearer to the transition zone. (Windbiel, 2017; Davidson, 2017).

Beyond Historical Large-Event Statistcs. A valid concern with this method could be that one would simply keep high alerts over the most active regions in the world and expect to get a high percentage of earthquakes within those areas compared to the entire planet. Such a method could conceivably determine the most active regions over five, ten, and twenty-year periods and make some good guesses about what parts of earth would yield the highest 'return' (number of earthquakes) for the size of the alert zone. In the present model, however, the alert zones are dynamic, and based on objective factors. Three of the four missed earthquakes during this period struck the region from Indonesia to the Solomon Islands- precisely the area one would need to cover in the aforementioned static-watch-zone scenario. Furthermore, the United States, Europe, Central America and New Zealand (all endured M6+ 'significant' earthquakes during the first 100 days while on highest alert) are not as active as South America, Japan, northern Oceania and westward faults through Indonesia, and would not have been on alert if only the most active regions were used in place of the described subterranean and atmospheric signals.

Mechanism of Action. At this time, the veracity of the pre-siesmic signals is more-easily understood than the mechanism of action- just like our ancestors could predict the movements of the celestial sights but misunderstood them to be living gods. It is uncertain whether the signals in this model are independently triggering the subsequent crustal earthquakes or are merely coincident symptoms in the progression of a larger process. The nature of the atmospheric signals used here, the nature *and location* of deep earthquakes, and the chemical composition within the mantle indicate that electromagnetism is a possible path to understanding the mechanisms of action triggering these events. A hypothesis expressing this mechanism is presented in part II of this communication.

Acknowledgements: The author would like to acknowledge Scott C. Windbiel for helping introduce Blot's work to us, and for being the first to actively discuss deep earthquake patterns near the transition zone beneath Oceania and their relation to crustal earthquakes across the western equatorial ring of fire. An automated Blot echo/pressure map program has been developed by 9RESE (9RESE.com) and is a free tool available at QuakeWatch.net/PredictionCenter. The founder of 9RESE, Todd Cleckner, was also instrumental in the discovery of the patterns relating to surface wind flow. Dong Choi has been a leading proponent of the science of seismic forecasting, and his publication, New Concepts in Global Tectonics Journal (ncgt.org), houses a disproportionately large number of the existing Blot-related works, and is both open access and open-minded. The ongoing work has included numerous advice and research from the collective of 'Suspicious0bservers,' a group of ~300,000 (as of 2017) science enthusiasts that come together to learn about, experience, and engage with solar-terrestrial, meteorological and geophysical subjects.

References:

Becken et al., Correlation between deep fluids, tremor and creep along the central San Andreas fault. *Nature* (2011)

Blot, C., *Publ. B.C.I.S. Series A., Travaux Scientifiques Fasc.*, **23**, 103 (August, 1963)

Blot, C. Volcanisme et sismicité dans les arcs insulaires. *Prévision De Ces Phénomènes* (1976)

Blot, C., Choi, D., and Grover, J. Energy transmission from deep to shallow earthquakes: a phenomenon applied to Japan. *NCGT Newsletter* (2003)

Choi D. and Casey J. Blot's Energy Transmigration Law and the September 2015 M8.3 Chile Earthquake. *New Concepts in Global Tectonics Journal* (2015)

Davidson, B., Holloman, C., U-yen, K., Relationship Between M8+ Earthquake Occurrences and the Solar Polar Magnetic Fields. *New Concepts in Global Tectonics Journal*, (September 2015)

Davidson, B., A Surge and Short-Term Peak in Northern Solar Polar Field Magnetism Prior to the M8.3 Earthquake Near Chile on September 16, 2015. *New Concepts in Global Tectonics Journal*, (September 2015)

Davidson, B., Earthquake Forecasts Record, The Earthquake Prediction Center at QuakeWatch.net (2017) docs.google.com/document/d/1zRUPkFrofDO7HF41pqvg6SXTJugNGtsszqaweF43HP0/edit?usp=sharing

De Santis et al., Potential earthquake precursory pattern from space: The 2015 Nepal event as seen by magnetic Swarm satellites. Earth and Planetary Science Letters (2017)

Fidani et al., A Study of the Correlation between Earthquakes and NOAA Satellite Energetic Particle Bursts. *Remote Sensing* (2010)

Giacco, F., Saggesse, L., de Archangelis, L., Lippielo, E., Pica Ciamarra, M., Dynamic Weakening by Acoustic Fluidization during Stick-Slip Motion. *Physical Review Letters* (2015)

Gregori, G. Migration of Foreshocks and/or Volcanic Eruptions: The "Blot's Migration Law". *New Concepts in Global Tectonics Journal* (2015)

Grover, J.C. Forecasting of Earthquakes—Correlation between Deep Foci and Shallow Events in Melanesia. *Nature* (1967)

Grover, J.C. Implications of blot's theory for the prediction of volcanic eruptions and earthquakes. *Geoexploration* (1974)

Hayakawa, M. Earthquake Prediction with Radio Techniques. (Book). *John Wiley & Sons,* ISBN 1118770161, 9781118770160 (2016)

Hill, R. D., Spherical capacitor hypothesis of the earth's electric field. Jour. *Pure and Applied Geophysics* (1971)

Iidaka et al., Large heterogeneous structure beneath the Atotsugawa Fault, central Japan, revealed by seismic refraction and reflection experiments. *Tectonophysics* (2015)
Johnston et al., Magnetic field observations in the near-field the 28 June 1992 M7.3 Landers, California earthquake. *Bull. Seis. Soc. Am.* (1994)
Kamogawa, M. and Kakinami, Y., Is an ionospheric electron enhancement preceding the 2011 Tohoku-Oki earthquake a precursor? *Jour. Geophys Res Space Physics* (2013)
Khachikyan et al., Solar modulation of earthquake occurrence in areas penetrated by L of 2.0 populated by anomalous cosmic rays. *40th COSPAR Scientific Assembly:* Abstract C4.1-49-14. (2014)
Lal and Bhagavathiammal., Association between earthquake and equatorial waves in outgoing longwave radiation over southeast Asia. *Indian Journal of Radio and Space Physics* (2016)
Morrow et al., Low resistivity and permeability in actively deforming shear zones on the San Andreas Fault at SAFOD. *Journal of Geophysical Research* (2015)
Namgaladze, A.A., Earthquakes and Global Electrical Circuit. *Russ. Jour. Physical Chemistry* (2013)
Namgaladze et al., Ionospheric total electron content variations observed before earthquakes: Possible physical mechanism and modeling. *Proc. MSTU* (2009)
Prakesh et al., Outgoing longwave radiation (OLR) from Kalpana satellite prior to Nepal earthquake of April 25, 2015 and its largest aftershock. *IJRET* (2015)
Pulinets, S., 2014. Electromagnetic Effects in the Atmosphere, Ionosphere and Magnetosphere Initiated by the Earthquake Preparation Process. General Assembly and Scientific Symposium (URSI GASS) Conference August 2014.
Rycroft, M.J., Electrical processes coupling the atmosphere and ionosphere: An overview. *Jour. Atmos, Sol,-Terr, Phys* (2006)
Scoville et al., Pre-Earthquake Magnetic Pulses. *Nat. Hazards Earth Syst. Sci.* (2015)
Sorokin et al., Formation Mechanism of the Lower-Ionosphere Disturbances by the Atmospheric Electric Current over a Seismic Region. *Jour. Atmos. Sol.-Terr. Phys.* (2006)
Ustundag et al., Multilayer Capacitor Model of the Earth's Upper Crust. *Turk J Elec Engin*, (2005)
Venkatanathan and Natyaganov., Outgoing longwave radiation as pre-seismic signals: preliminary results of 24 September 2013 (M7.7) earthquake. *CURRENT SCIENCE* (2014)
Whiteside, L. S., and Y. Ben-Zion, Universal triggering patterns in earthquake sequences and the use of triggering for earthquake prediction (abstract), *Eos. Trans. AGU*, 76,532, 1995.
Windbiel, S. https://plus.google.com/117300779230803580292 Public Access/Open Source Seismic Forecasting using what this communication describes as "Blot echoes."
Yao et al., Analysis of pre-earthquake ionospheric anomalies before the global M = 7.0+ earthquakes in 2010. *Nat Hazards Earth Syst. Sci.* (2012)
Zolotov et al., TEC anomalies before the Haiti Jan. 12, 2010 and China May 12, 2008 earthquakes. *38th COSPAR Scientific Assembly*: 5. (2010)